

FULL-SCALE WIND TUNNEL TEST OF A UH-60 INDIVIDUAL BLADE CONTROL SYSTEM FOR PERFORMANCE IMPROVEMENT AND VIBRATION, LOADS, AND NOISE CONTROL

Thomas R. Norman and Colin Theodore
NASA Ames Research Center, Moffett Field, CA

Patrick Shinoda
Aeroflightdynamics Directorate (AMRDEC)
U.S. Army Research, Development, and Engineering Command
Ames Research Center, Moffett Field, CA

Daniel Fuerst and Uwe T. P. Arnold
ZF Luftfahrttechnik GmbH, Kassel-Calden, Germany

Stephen Makinen, Peter Lorber, and John O'Neill
Sikorsky Aircraft Corporation, Stratford, CT

ABSTRACT

A full-scale wind tunnel test of a UH-60A rotor was recently completed in the National Full-Scale Aerodynamics Complex 40- by 80-Foot Wind Tunnel to evaluate the potential of Individual Blade Control (IBC) to improve performance; to reduce vibration, loads, and noise; to affect flight control characteristics; and to perform reconfiguration and in-flight tuning tasks. This test was the culmination of a long-term collaborative wind tunnel test program between NASA, U.S. Army, Sikorsky Aircraft Corporation, and ZF Luftfahrttechnik GmbH (ZFL). Initial test results are promising, with demonstrated rotor power reductions (up to 5%), multi-parameter hub load reductions, multi-frequency pitch link load reductions, and in-plane noise reductions. Additional results indicate the benefits of IBC for in-flight tuning and show minimal coupling of IBC with UH-60A rotor flight dynamics.

NOTATION

AF_BD_SH	Axial force at rotor hub, shaft axis (calculated from rotating shaft gages)
A0,i	IBC blade pitch offset of blade i
Ai	i/rev IBC amplitude
C _l /σ	Rotor lift coefficient divided by rotor solidity
IBC _i FORCE	Force of IBC actuator i
L/D _e	Rotor lift divided by equivalent drag
NF_BD_B1	Normal force at rotor hub, shaft axis (calculated from rotor balance)
PHASE _i	i/rev IBC phase angle
PM_BD_SH	Pitching moment at rotor hub, shaft axis (calculated from rotating shaft gages)
PM_BAL_B1	Pitching moment at balance, shaft axis (calculated from rotor balance)
RM_BD_SH	Rolling moment at rotor hub, shaft axis (calculated from rotating shaft gages)
SF_BAL_B1	Side force at balance, shaft axis (calculated from rotor balance)

α_s	Rotor shaft angle measured from vertical, positive aft, deg
μ	Advance ratio

INTRODUCTION

A full-scale wind tunnel test was recently conducted (March 2009) in the National Full-Scale Aerodynamics Complex (NFAC) 40- by 80-Foot Wind Tunnel to evaluate the potential of an individual blade control (IBC) system to improve rotor performance and reduce vibrations, loads, and noise for a UH-60A rotor system. This test was the culmination of a long-term collaborative effort between NASA, U.S. Army, Sikorsky Aircraft Corporation, and ZF Luftfahrttechnik GmbH (ZFL) to demonstrate the benefits of IBC for a UH-60A rotor.

The first test of this collaborative effort was completed in the NFAC 80- by 120-Foot Wind Tunnel in September 2001. A UH-60A rotor and IBC system were mounted on the NFAC Large Rotor Test Apparatus (LRTA) and tested in forward flight at speeds up to 85 knots. A complete description of the LRTA, wind tunnel installation, and UH-60A rotor hardware is provided in Ref. 1. During this test, open-loop IBC system functionality was established and

Presented at the American Helicopter Society 65th Annual Forum, Grapevine, TX, May 27-29, 2009. This is a work of the U.S. government and is not subject to copyright protection in the U.S.

low-speed vibration and acoustic data were acquired. Substantial vibratory load reductions (up to 80%) and BVI noise reductions (up to 12 dB at some microphones) were realized with specific IBC inputs (Ref. 2).

For the current test, the same UH-60A rotor and IBC system were tested in the 40- by 80-Foot Wind Tunnel at speeds up to 170 knots. Figure 1 shows the LRTA and rotor installed in the test section. As in the previous test, the ability of IBC to reduce vibration, loads, and noise was evaluated, with particular emphasis on reductions at high forward flight speeds. In addition, the effects of IBC on flight control characteristics and the ability of IBC to perform in-flight tuning and reconfiguration tasks were investigated. The primary objective of this test, however, was to demonstrate the ability of IBC to improve rotor performance.



Figure 1. UH-60A Rotor System installed on the Large Rotor Test Apparatus in the NFAC 40-by 80-Foot Wind Tunnel.

Previous wind tunnel experiments (Ref. 3, 4), flight experiments (Ref. 5) and analytical efforts (Ref. 6, 7) have suggested that IBC may be capable of reducing the power required at specific flight conditions. Unfortunately, some of the experimental results have been questioned because of uncertainties associated with resetting rotor trim (particularly propulsive force) following application of IBC. For the current test, these uncertainties have been addressed by implementing a closed-loop trim control system to automatically adjust the fixed-system controls to match specific rotor trim targets. A description of this system and the trim methods used is provided in this paper.

In addition to the trim control system, a key feature of the current test was the use of closed-loop IBC controllers for vibration and load reduction. Open-loop recursive system identification was used to estimate the underlying plant model for the initialization of these closed-loop controllers, and both adaptive and non-adaptive algorithms were used to search for the optimal mix of IBC harmonics. To enable this

testing, ZFL modified the original IBC control hardware and software to accept externally-generated, closed-loop control commands and to provide a platform for the integration of closed-loop algorithms.

The current paper provides an overview of the recently completed wind tunnel test and includes detailed descriptions of the IBC and wind tunnel hardware, instrumentation and data systems, IBC closed-loop controller, and closed-loop trim controller. A discussion of the test objectives and approach and initial results of the effects of IBC are then presented.

DESCRIPTION OF THE EXPERIMENT

The test was conducted in the NFAC 40- by 80-Foot Wind Tunnel using a Sikorsky Aircraft UH-60A rotor system mounted on the LRTA. Figure 1 shows the model installed in the wind tunnel. In the following sections, detailed information is provided describing the experiment (including test hardware), instrumentation, data acquisition and reduction systems, rotor control systems, and standard test procedures.

Hardware

NFAC 40- by 80-Foot Wind Tunnel

The 40- by 80-Foot Wind Tunnel is part of the National Full-Scale Aerodynamics Complex (NFAC) located at NASA Ames Research Center. The NFAC, closed in 2003, was recently reactivated by the U.S. Air Force under a long-term lease agreement with NASA and is managed and operated by the U.S. Air Force's Arnold Engineering Development Center (AEDC). The current test program represents the second rotor test in the facility since its reactivation and the first to use many of its upgraded capabilities. The tunnel has a closed test section with semicircular sides, a closed-circuit air return passage, and is lined with sound-absorbing material to reduce acoustic reflections. The actual test section dimensions are 39 feet high, 79 feet wide, and 80 feet long and the maximum test section velocity is approximately 300 knots.

NFAC LRTA Test Stand

The LRTA (Fig. 1) is a special-purpose drive and support system designed to test helicopters and tilt rotors in the NFAC. Its primary design features include 1) a drive system powered by two 3000 HP motors, 2) a five-component rotor balance to measure steady and unsteady rotor hub loads, along with an instrumented flex-coupling to measure rotor torque, 3) a six-component fuselage load-cell system to measure steady fuselage loads, 4) a complete rotor control system with primary and dynamic actuator control, and 5) an output shaft assembly with a replaceable upper shaft to allow

different rotor systems to be mounted. A detailed description of the LRTA and its capabilities can be found in Ref. 1.

Of particular note for this test is the LRTA rotor control system. Non-rotating swashplate control is provided through three identical actuator assemblies, each of which includes both primary and dynamic actuators. The primary actuators are high-authority/low-speed ball-screw electric actuators and are used to provide primary control of rotor blade pitch by tilting the swashplate. The dynamic actuators are low-authority ($\pm 2^\circ$ of blade pitch for this test), high-speed rotary-hydraulic actuators and are used to provide time-varying perturbations to the swashplate. Each primary/dynamic actuator pair operates in series to provide the total swashplate actuation.

Control of the actuator assemblies is provided through two separate, and somewhat independent, position control systems, the Primary Control Console (PCC) and the Dynamic Control Console (DCC). The PCC provides the operator with low-bandwidth control of the three linear electric (primary) actuators. This position control is achieved by driving three control rod linkages, whose positions define the orientation of the swashplate; and, hence, rotor blade collective and cyclic pitch. The DCC provides the operator with control of the three rotary-hydraulic (dynamic) actuators to provide oscillatory pitch-angle perturbations about the nominal angle set by the PCC. Internal DCC capabilities allow control inputs to a single actuator or to any of the helicopter's control axes (collective, lateral or longitudinal). In addition to these internal capabilities, externally generated signals can be used to drive the actuators. For this test, the dynamic actuators were controlled with an external control system (designated the Trim Control System) through the DCC external inputs.

The LRTA was mounted on three struts as shown in Fig. 1, allowing for an angle-of-attack range of 0° to -15° . This installation put the rotor plane (at $\alpha_S = 0^\circ$) 10.9 inches above the tunnel centerline (20.4 ft above the acoustically treated floor).

Rotating Hardware

The rotating hardware used during this program was predominantly UH-60A flight hardware, with the exception of the instrumentation hat and those components necessary for IBC actuator operation. A schematic of this hardware is shown in Fig. 2. The interface locations between the UH-60A rotor and LRTA occurred at 1) the UH-60 shaft extension, 2) the bottom of the swashplate guide and, 3) the non-rotating swashplate. The interface locations between the UH-60A rotor and the IBC hardware occurred at 1) the top of the hub, 2) the bottom of the upper pressure plate and, of course, 3) the pitch link locations. The instrumentation hat

was mounted on top of the IBC adapter on top of the hub. Details of the rotor and IBC hardware are presented below.

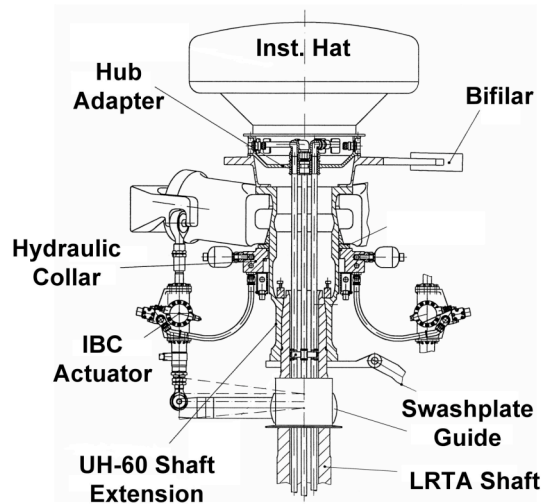


Figure 2. Schematic of rotating hardware.

UH-60A Rotor System. The UH-60A is a four-bladed, articulated rotor system consisting of four subsystems: hub, blade pitch controls, bifilar vibration absorber, and main rotor blades. The four titanium-spar main rotor blades attach to spindles that are retained (by elastomeric bearings) to a one-piece titanium hub. These bearings permit blade flapwise and lead-lag motion. Main rotor dampers are installed between each of the main rotor spindles and the hub to restrain lead-lag motion of the main rotor blades during rotation and to absorb rotor head starting loads. Blade pitch is controlled through adjustable pitch links that are moved by the swashplate. The bifilar vibration absorber is designed to reduce rotor vibration at the rotor head. The absorber is mounted on top of the hub and consists of a four-arm plate with attached weights. The bifilar weights were not installed for this test, however, so the effects of IBC on vibration could be studied in isolation. A summary of relevant main rotor system parameters is presented in Table 1 and Ref. 8.

Table 1. UH-60 Rotor Parameters

Parameter	Value
Number of blades	4
Radius, ft	26.83
Nominal chord, in	20.9
Equivalent blade twist, deg	-18
Blade tip sweep, deg aft	20
Geometric solidity ratio	.0826
Airfoil section designation	SC1095/SC1095R8
Thickness, % chord	9.5
100% RPM	258

The specific blades used in this test program constitute 4 out of the set of 5 matched rotor blades flown during the UH-60A Airloads Program (Ref. 9). Of these five original blades, two were heavily instrumented by Sikorsky Aircraft under NASA contract: one with 242 pressure transducers and one with a mix of strain-gages and accelerometers. The pressure-instrumented blade was the one blade not used during this program. Details of the rotor blade instrumentation are provided in a later section.

IBC Hardware. The IBC system developed for the UH-60 replaces the normally rigid pitch links of the rotor with servohydraulic actuators. These actuators allow the blade pitch of each rotor blade to be changed independently of each other and were designed with the capability to provide up to $\pm 6.0^\circ$ at 2/rev frequency and up to $\pm 1.6^\circ$ at 7/rev frequency. For this test the actuator travel was mechanically limited to $\pm 3.0^\circ$. Reference 10 provides a full discussion of the actuator characteristics, the automatic emergency shutdown feature, the development program, qualification testing, and the installation onto the LRTA. Figure 3 shows a schematic of one IBC actuator, while Fig. 4 shows an actuator installed on the LRTA.

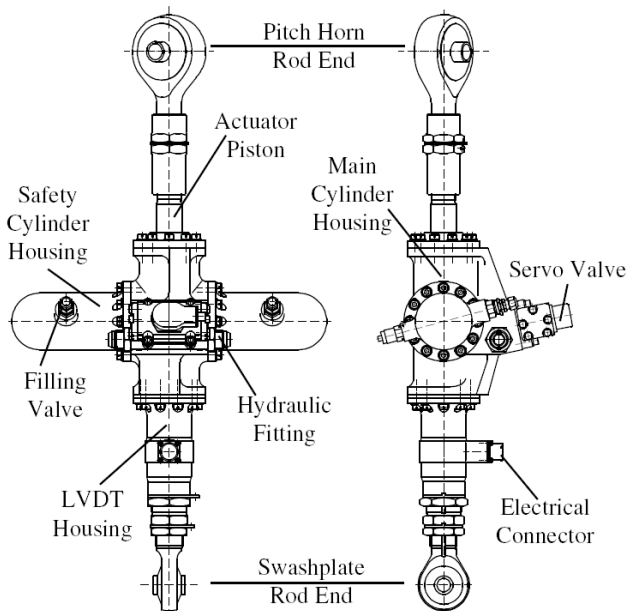


Figure 3. IBC actuator schematic.

Instrumentation

A total of 82 rotor and IBC parameters (Table 2) and 101 LRTA and wind tunnel parameters (Table 3) were measured and acquired as part of this test program. The following section briefly describes a few of the key measurements from these parameter groups.

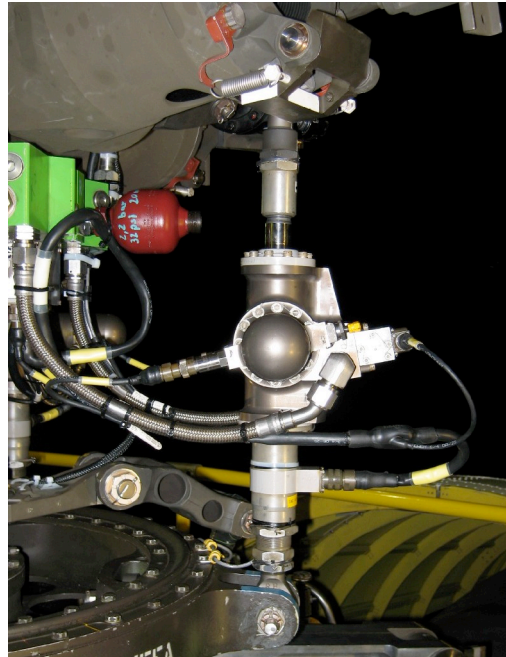


Figure 4. IBC actuator installed on UH-60A rotor.

Table 2. Rotor and IBC Parameters

Measurement Type	Number of gages
Spindle, hub arm, blade lug stresses	10
Rotating scissors, damper loads	4
Hub accelerometers	3
Pitch, flap and lag angles	12
Blade normal, flap, and torsion moments	24
Blade stress	5
Shaft gages (Moments and stress)	8
IBC actuator force	4
IBC actuator positions and commands	12

Table 3. LRTA and Wind Tunnel Parameters

Measurement Type	Number of gages
Balance and Flex-coupling forces and moments	28
Balance and Flex-coupling temps	14
Stationary pushrods, scissors and swashplate guide (forces/moments)	8
Control System Positions/Commands	15
Fuselage loadcells	6
Tunnel Pressures and temperatures	17
Model angles and RPM	3
Microphones	10

Rotor and IBC Parameters

Two of the four rotor blades carried instrumentation. Blade 1, the heavily instrumented strain-gage blade used during the flight test phase of the NASA/Army UH-60A Airloads Program, contained 22 strain gages measuring torsion, normal bending, and edgewise bending. Blade 3 was instrumented with 2 strain gages at the blade root as back-ups for critical Blade 1 measurements. Force measurements were acquired for the two rotating scissors and two of the four dampers. The accelerations of the instrumentation hat (attached to the top of the hub) were measured by 3 orthogonal accelerometers. The hub instrumentation also included specially designed blade motion measurement devices used to determine blade flap, lag, and pitch angles on each blade (see Ref. 9 for details). The rotor shaft was instrumented with eight strain gages, four to measure shaft stress and four to measure shaft moment. These latter 4 gages were positioned to allow determination of the rotating forces and moments at the hub.

The IBC actuator positions were measured using two LVDTs (Linear Variable Differential Transducer) per actuator. One of these transducers was used to close the actuator position control loops and the second one was used by a monitoring system. Additionally, each actuator was instrumented with strain gages to measure actuator axial force (equivalent to pitch link load).

LRTA and Wind Tunnel Parameters

As discussed in Ref. 1, a five-component rotor balance with steady and dynamic load measuring capability is integrated into the LRTA. The four balance flexures are instrumented with 12 primary gages and 12 back-up gages which can be combined to determine rotor normal, axial and side forces, together with the rotor pitching and rolling moments. The rotor shaft has an in-line flex-coupling, which is instrumented to redundantly measure rotor torque, residual power-train normal force, and temperature. The LRTA chassis is linked to the aerodynamic fairing with a six-component fuselage load-cell system to measure steady fuselage loads.

A total of 8 strain gage measurements were made on stationary control hardware, including three on the stationary pushrods, one on the stationary scissors, and four on the swashplate guide. Two displacement measurements for each primary actuator and two displacement measurements for each dynamic actuator (for a total of 12 measurements) were also acquired.

Acoustic data were acquired using 10 microphones mounted at the fixed positions identified in Fig. 5. Microphones 1,2,6 and 7 were located under the advancing side of the rotor at positions of estimated high Blade Vortex Interaction (BVI) noise, and/or to coincide with similarly positioned

microphones during previous tests. The remaining microphones were placed forward of the model to measure in-plane, low frequency rotor source noise. The microphone coordinates are given in Table 4. The coordinate system is centered on the rotor hub when the shaft angle is set to zero ($\alpha_s = 0^\circ$).

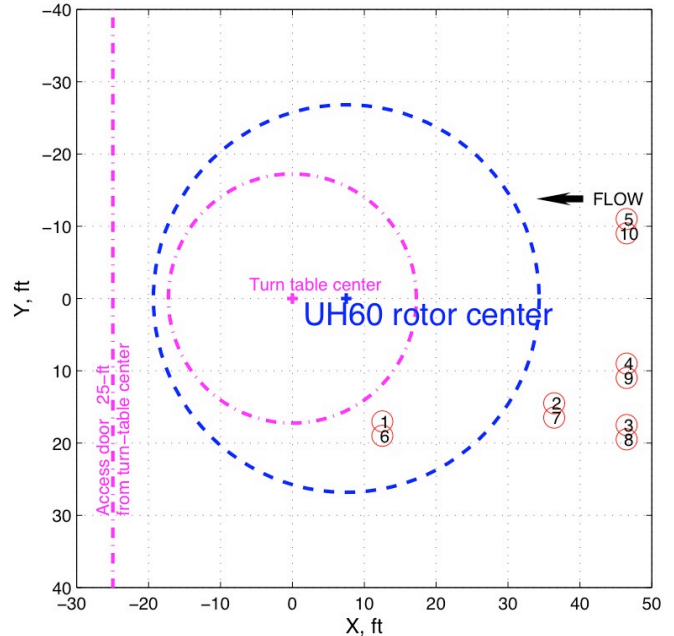


Figure 5. Orientation of microphones and rotor in 40- by 80-Foot test section.

Table 4. Microphone Positions

Mic #	x	y	z
1	5.33	17.50	14.17
2	28.83	15.58	14.17
3	39.25	17.83	4.92
4	39.25	9.42	4.92
5	39.33	-9.83	4.92
6	5.33	17.83	14.17
7	28.83	15.91	14.17
8	39.25	18.16	4.92
9	39.25	9.75	4.92
10	39.00	-9.50	4.92

*All dimensions in feet, origin at rotor hub except z-dimension is height from floor.

Data Acquisition and Reduction

Six separate systems were used during this test program to provide signal conditioning and/or to digitize, reduce, and store data. These systems included the NFAC Data Acquisition System (NFAC DAS), the Data Transfer Computer (DTC), the Fatigue Monitoring System, the IBC Control System, the Trim Control System, and the LRTA Rotor Control Console. Figure 6 shows a block diagram of

how these systems interface with one another. A short description of each system is provided in the following section.

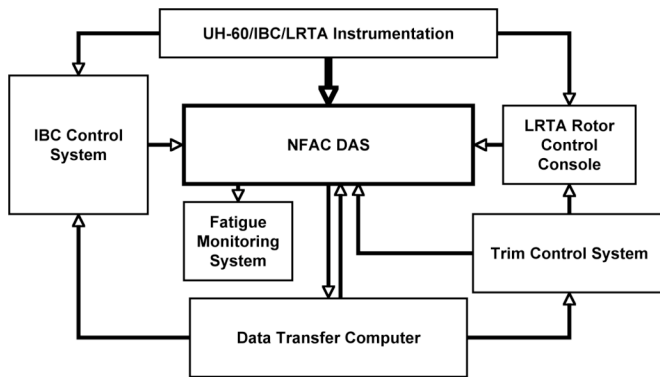


Figure 6. Block diagram of data acquisition and reduction systems.

NFAC DAS

The NFAC DAS was the primary data acquisition system for this test and nearly all data were ultimately sent to this system for digitization and storage. The NFAC DAS is a new data system, developed by the Air Force for tests to be conducted in the NFAC. A detailed description of this new system can be found in Ref. 11. Key features include a large available channel count, variable sample rates based on the rotor N/rev and synchronized with each other, and variable length data records, up to 256 revolutions. In addition, this system allows multiple data points to be recorded consecutively, effectively increasing the amount of time continuous data can be recorded beyond the maximum data point length. The NFAC DAS uses an oversample/re-sample technique to ensure all data are aligned with the rotor azimuth position. Corrections for any time delay caused by the NFAC analog anti-aliasing filters are incorporated during the re-sample process. For this test, most data were sampled at a rate of 256 samples/rev; acoustic data were sampled at 2048 samples/rev. Data were acquired for a range of sample durations, ranging from 32 to 256 revolutions, depending on the specific test objective. The multiple point capability was also used to record up to 200 seconds of continuous data split into four 256-revolution data points. The system also provided both real-time and post-point data reduction and processing capabilities.

Data Transfer Computer

The Data Transfer Computer (DTC) was designed to acquire analog data, compute derived parameters, and provide the derived data in analog form to the IBC and Trim Control Systems in near real-time. All analog input data were provided through the NFAC DAS amplifiers, sent through 100 Hz anti-aliasing filters, and digitized by the National Instruments RT-based DTC at 256 samples/rev. These data

were simultaneously sampled, converted to engineering units, combined together into the desired derived parameters, and then converted to analog output with a total delay of one-half the sampling period. These analog data were then sent to the two control systems as well as to the NFAC DAS for acquisition and storage. The derived data included rotor balance forces and moments (in the balance axis and hub axis systems) as well as hub axis loads derived from the shaft bending gages.

Fatigue Monitoring System

To meet the test objectives of this program, it was necessary to track the accumulation of fatigue damage on various rotor and LRTA components. An on-line Fatigue Monitoring System was developed to accomplish this task. This new system was designed to measure, calculate and display the magnitude of each fatigue-critical parameter for each rotor revolution, in real time. The developed system was capable of recording up to 32 input measurements; derived parameters could be calculated from any of these inputs. The rotor 1/rev signal triggered acquisition of data samples equally spaced about the azimuth. The vibratory load was then calculated from the maximum and minimum values measured during the current rotor revolution, compared to the endurance limit for each parameter, and recorded if the endurance limit was exceeded. Endurance limits, established from fatigue tests, were adjusted as necessary to account for the maximum predicted test steady load. The on-line screen display consisted of a series of bins representing increasing magnitude above the endurance limit. For each exceedance cycle, the appropriate bin was indexed. The Fatigue Monitor display showed the total bin count during the run as well as estimates of fatigue damage (in % of life used) for two user-specified time periods. Corrections to the total damage estimate were necessary for higher frequency loading.

IBC Control System

In addition to its primary task of controlling the IBC actuators (in either open- or closed-loop mode), the IBC Control System was designed to provide primary signal conditioning for all IBC parameters (including position and force measurements) and to provide data acquisition, reduction, and analysis capabilities. Data were acquired at different sample rates for variable data record lengths, depending on the test objective and procedure. Data records over 1000 revolutions in length were recorded for some test points. All IBC parameters as well as those analog values provided by the DTC were A/D-converted at a sample rate of 128 samples/rev and captured together with additional internal parameters at this sample rate. No additional anti-aliasing filters were used prior to digitization. Data synchronization was performed during post processing using a 1/rev trigger signal. To enable IBC closed-loop capabilities, substantial real-time data reduction capabilities

(e.g. calculation of N/rev components of vibrations, loads, etc.) were implemented within the IBC system. These calculations were updated only once per revolution and hence the corresponding data were also acquired at this rate. Other important real-time calculations, like the recursive system identification or the closed-loop calculation of IBC commands, were implemented with adjustable sample rate and input data for these tasks were sampled at this rate. Analog outputs of many of the IBC parameters (including forces and positions), as well a limited number of derived parameters, were provided to the NFAC DAS for final digitization and storage.

Trim Control System

In addition to its primary task of controlling the LRTA dynamic actuators for trim control, the Trim Control System was designed to provide data acquisition, reduction, and analysis capabilities. Analog input data from the DTC were sent through a 100 Hz anti-aliasing filter before being digitized by the Trim Control System. The Trim Control System cycled at 100Hz and continuously acquired data at this rate for an entire test run (up to 3-4 hours). Recorded data included all input and output voltage and engineering unit channels, and internal trim control parameters used for development and validation of the controller. Data records for each test point were extracted in post-run data processing. Analog outputs of many of the system parameters, including actuator commands, were also provided to the NFAC DAS for final digitization and storage.

LRTA Rotor Control Console

The LRTA Rotor Control Console provided the primary signal conditioning for both primary and dynamic LRTA actuator positions. In addition, the console provided the primary signal conditioning for two of the four blade flap measurements as well as two of the four blade pitch measurements. Anti-aliasing filters were set to 500 Hz for all blade gages. Analog outputs of all these measurements, in addition to dynamic actuator command positions, were provided to the NFAC DAS for final digitization and storage.

Rotor Control Systems

Three separate rotor control systems (the LRTA Primary Control System, the Trim Control System, and the IBC Control System) were utilized during this test program, with each system controlling an independent set of actuators. The LRTA Primary Control System provided open-loop control of the LRTA primary actuators (and swashplate) and was the standard method for manual control of the rotor system. The Trim Control System provided open- and closed-loop control of the LRTA dynamic actuators (and swashplate) to precisely set and maintain rotor trim or to dynamically excite

the rotor system with frequency sweep (chirp) inputs. The IBC Control System provided open- and closed-loop control of the rotating IBC actuators. The latter two control systems were developed specifically for this test program.

Figure 7 shows a simplified block diagram of the three rotor control systems and how they interact. The general functionality of each system is described below. More complete descriptions of the Trim Control and IBC Control Systems are provided in the Appendix.

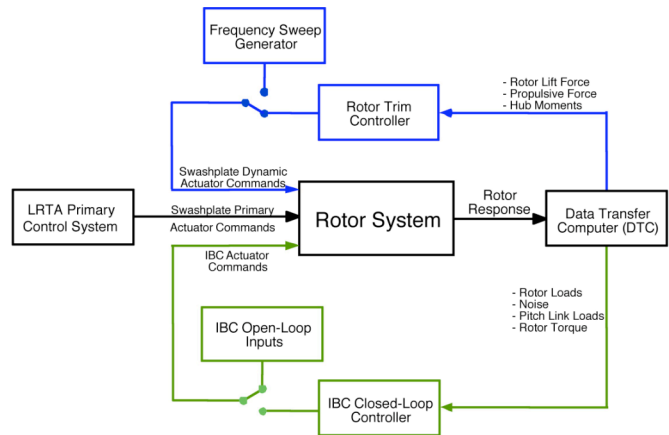


Figure 7. Simplified block diagram of three rotor control systems.

LRTA Primary Control System

Control of the primary actuators was provided through the LRTA Primary Control Console (PCC), discussed above and in Ref. 1. The PCC provided the operator with low-bandwidth control of the three linear electric (primary) actuators and allowed the operator to manually trim the rotor based on displays of rotor force and moment coefficients, and rotor flapping. Due to the manual nature of this control system, it was sometimes difficult to precisely set up on rotor trim conditions.

Trim Control System

Control of the LRTA dynamic actuators was provided through the Trim Control System (Trim Controller). This control system allowed the rotor trim state to be set more precisely and quickly than was possible with the rotor operator driving the swashplate primary actuators through the PCC. The Trim Controller also maintained the desired trim condition through changes in IBC actuation and long-period transients in wind tunnel flow. A frequency sweep (chirp) generator function was built into the trim controller logic to allow rotor dynamic response data to be collected.

Two main trim control methods were built into the rotor trim controller. The first trim method controlled the rotor lift and hub pitching and rolling moments through swashplate collective, longitudinal cyclic, and lateral cyclic pitch

commands to the swashplate dynamic actuators. The rotor propulsive force was controlled through changes to the model shaft angle that were applied manually. The trim controller calculated the shaft angle change required to obtain the desired propulsive force based on a look-up table of the propulsive force sensitivity to shaft angle change. Typically one or two shaft angle change iterations were required to converge on the desired rotor propulsive force.

The second trim method controlled the rotor lift, propulsive forces and hub rolling moment through swashplate collective and cyclic pitch commands to the swashplate dynamic actuators. This trim method was performed with the shaft angle fixed since the rotor propulsive force was controlled directly through swashplate inputs. The hub pitching moment was not controlled or used for feedback in this method. This second trim control method was much more time efficient than the first method since the rotor was trimmed and re-trimmed in a matter of seconds with swashplate inputs, whereas the first method required manual changes in model shaft angle which took considerably more time.

IBC Control System

Control of the IBC actuators was provided through the IBC Control System. The system architecture developed and used for this IBC wind tunnel test was based upon the IBC control system used in the earlier full-scale UH-60 IBC wind tunnel test (Ref. 1, 2, 10). The core system, including both the inner and intermediate control loops (Ref. 10) with their built-in safety features, was almost completely retained. However, modifications to the system were necessary in order to incorporate new IBC capabilities, including 1) IBC closed-loop, e.g. for N/rev vibration control, 2) individual blade 1/rev pitch commands, and 3) individual blade pitch offset commands. This was accomplished with the development of a separate outer loop, real-time control system.

The closed-loop control algorithms used to form the outer control loop for different objectives were based on the assumption that a quasi-static linear relationship between the outputs (e.g. harmonic components of measured vibrations) and the corresponding set of IBC inputs can describe the plant behavior accurately (linear T-matrix model, Ref. 12-16). The overall outer control loop consisted of two main tasks: 1) a system identification task to estimate the linear T-matrix model recursively in real-time and 2) a controller task to calculate IBC inputs to accomplish the desired objective. Two different methods were developed and implemented to accomplish the controller task.

IBC Operations and Trim Procedures

Both open- and closed-loop IBC operations were performed during this test program. An overview of each operation is provided below. Also included below are the rotor trim procedures using the Trim Controller.

IBC Open-loop Operation

The IBC control system could be configured to provide open-loop sweeps of IBC phase (for given frequency and amplitude) following a specified schedule. These sweeps could either be automatic, with the sweep duration and phase fade-in/fade-out characteristics set prior to the sweep; or manual, with movement to new phases controlled by the operator. The automatic mode was the most efficient, with the effects of phase on any measured parameter available soon after the completion of the sweep. However, the automatic mode variables had to be set carefully so the parameters of interest (i.e. power) had time to settle out before moving to the next IBC phase. The manual mode was slower but ensured that the transient effects of IBC phase changes were minimized. In addition, this mode was used for IBC amplitude sweeps at a single phase or for phase sweeps at higher amplitudes where loads or trim controller limits precluded the use of a complete automatic phase sweep.

Additionally, the IBC control system could be configured to automatically generate blade-pitch offset variations in a pre-defined schedule. These automatic open-loop IBC inputs were used to recursively identify the part of the T-Matrix model which was used for the closed-loop in-flight tuning application. And finally, any fixed combination of IBC command values could be configured manually by the operator and faded in.

IBC Closed-loop Operation

The IBC control system could also be configured to provide closed-loop control of specified parameters (or weighted combinations of parameters). Typically this closed-loop testing consisted of two parts: 1) a series of automatic open-loop sweeps to identify the T-matrix to be used by the closed-loop controller, and 2) application of a specified closed-loop algorithm (with fixed or adapting T-matrix) to control the desired parameter(s). The various parameters used to configure the controller and the system identification algorithm could be modified by a man-machine interface.

Rotor Trim Procedures

The procedure to trim the rotor system during this test was to first have the rotor operator get close to the desired condition using the LRTA primary actuators. Precise force and moment trim values were entered into the trim controller operator interface and the trim controller was activated in

'continuous' mode to drive the swashplate dynamic actuators to refine the rotor trim to the desired condition. The trim controller continually updated the swashplate commands to maintain the desired trim condition through changes in IBC actuation and long-period transients in wind tunnel flow.

When the trim controller was operated using the first trim method (with pitch moment control), the shaft angle was changed manually to trim to the desired propulsive force. This shaft angle change was calculated by the trim controller and called out to the LRTA model operator, who entered the shaft angle change manually. During this shaft angle change, the trim controller remained in 'continuous' mode to hold the rotor lift and hub pitch and roll moments at the desired values. When the trim controller was operated using the second trim method, the propulsive force was controlled directly through swashplate inputs and no shaft angle changes were required.

Note that of the two trim control methods described above, only the second method (without pitch moment control) could be used with the IBC system in automatic open-loop or closed-loop mode. Either method could be used with the IBC system in manual open-loop mode.

TEST OBJECTIVES AND INITIAL RESULTS

As stated earlier, the objectives of this test program were to evaluate the ability of IBC to improve performance; to reduce vibration, loads, and noise; to affect flight control characteristics; and to perform reconfiguration and in-flight tuning tasks. Detailed discussion of each of these objectives, including the test approach used, is provided in the following section. Also included in this section are some initial test results. Although these results should be considered preliminary (more analysis of the test data is required), it is not expected that the general conclusions will change.

Performance Improvement

The primary objective of this test was to evaluate the ability of IBC to improve the rotor performance of a UH-60A rotor at representative flight conditions. Meeting this objective requires comparison of rotor power and lift-to-equivalent drag ratio (L/D_e) at the same flight condition with and without IBC active. Since the 2/rev IBC inputs necessary for performance improvement can significantly alter the trim conditions (lift, propulsive force, hub moment), the NASA-developed Trim Controller (discussed above) was required to accurately reset trim during IBC operation.

To determine the preferred testing approach, IBC performance data were acquired at a single flight condition

using 1) two different trim control methods (with and without pitching moment control), and 2) two different IBC open-loop testing methods (manual and automatic). Comparisons of power reductions showed consistent results for both trim methods as well as both testing methods. This allowed the use of the most efficient trim method (without pitching moment control) and the most efficient IBC control method (automatic) whenever practical for the remainder of the test.

Data were acquired at 4 representative 1-g flight conditions to determine the effects of advance ratio on IBC performance. Similar data were acquired at 5 different thrust levels (for one advance ratio) to investigate the effects of thrust (and stall). At each condition, IBC phase and amplitude sweeps were conducted. Figures 8 and 9 provide example results for one flight condition ($C_1/\sigma=0.077$, $\mu=0.40$, $\alpha_s=-8.6^\circ$). In Fig. 8, data are shown from an automatic open-loop phase sweep (at 1° IBC amplitude) with the Trim Controller active. Power, lift, propulsive force and L/D_e variations (in % change) are plotted as a function of IBC phase angle. These results demonstrate the ability of the Trim Controller to keep lift and propulsive force nominally constant as the IBC phase is varied. In addition, the reduction of rotor power (-3.3%) and increase of L/D_e (5.4%) are clearly seen, with maximum benefit at phase angles between 210° and 240° . Figure 9 shows the effect of IBC amplitude on power reduction for this same flight condition at a single IBC phase of 225° . These data show a maximum power reduction of 5.0% and maximum L/D_e improvement of 8.6% at IBC amplitudes of 2.0° .

Complete results from this and other flight conditions will be available following additional post-processing and analysis.

Hub Load/Vibration Reduction

The hub load/vibration objective was to measure the effects of open-loop IBC on 4/rev rotor hub loads and then evaluate the ability to reduce them (individually and collectively) using closed-loop control. Open-loop data were acquired at three representative flight conditions, including one at high thrust. Closed-loop testing was then completed for two of these conditions. This latter testing included various combinations of controlled parameters, weighting functions, and IBC input frequencies.

Figures 10 and 11 show example open-loop results for one flight condition (Lift=17,700 lb, $\mu=0.25$, $\alpha_s=-3.0^\circ$). These figures plot the amplitudes and phase angles of the 4/rev hub forces and moments for phase sweeps at IBC frequencies of 3/rev (Fig. 10) and 4/rev (Fig. 11). These open-loop data demonstrate the relationship between IBC input and hub load response and were used to identify, in real time, the T-matrix necessary for operation of the closed-loop controller.

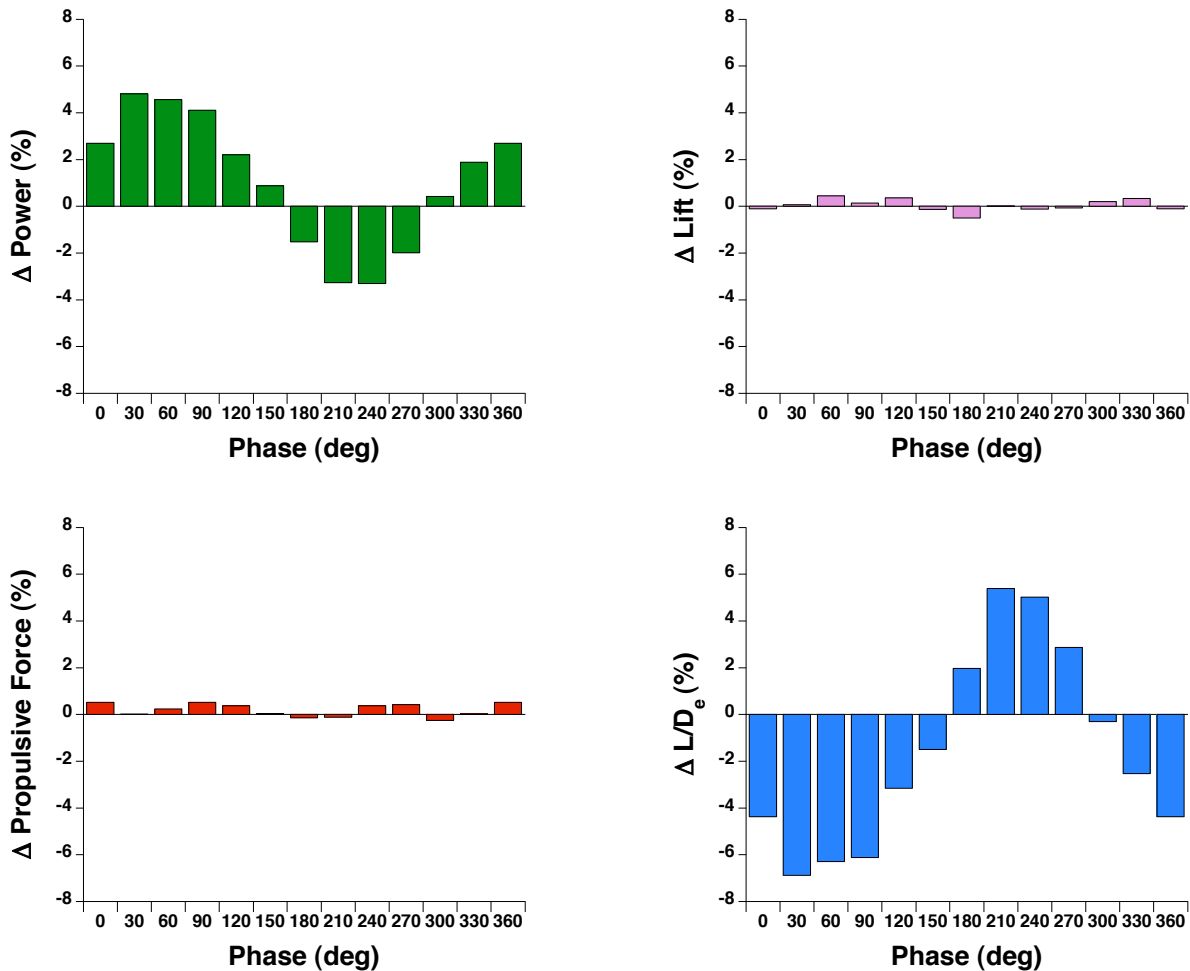


Figure 8. Performance results from 2/rev automatic IBC phase sweep (1° amplitude) with Trim Controller active, $C_l/\sigma=0.077$, $\mu=0.40$, $\alpha_s=-8.6^\circ$.

Figures 12 and 13 provide example closed-loop results for this same flight condition. Figure 12 demonstrates how a single parameter (4/rev hub pitching moment in this case) can essentially be eliminated using IBC (1.5° of 3/rev input). The upper two charts show the time history of the 3/rev IBC amplitude and the corresponding IBC phase during the test sequence and the lower chart shows the variation of the 4/rev hub pitching moment amplitude. As indicated by the time history of the IBC amplitude, the test sequence consists of an initial reference portion (first 5 sample points), a closed-loop IBC operation portion, and a final reference portion (last 5 sample points). Each sample point represents data calculated from the last 12 rotor revolutions. Figure 13 shows the closed-loop results when attempting to minimize the 4/rev component of three parameters using both 3/rev and 4/rev IBC input. The 4/rev controlled parameters (hub pitching moment, rolling moment, and normal force), as well

as one uncontrolled parameter (axial force), are shown. For this case, the IBC actuation was artificially limited to prevent load parameters, not included in the cost function, from increasing to values greater than the do-not-exceed limits for this experiment. Thus a true closed-loop solution was not obtained. Nonetheless, the results indicate that simultaneous reduction of multiple hub loads is possible with IBC.

Pitch Link Load Reduction

The pitch link load objective was to demonstrate the ability of closed-loop IBC to reduce the prominent pitch link load harmonics (2/rev – 5/rev) and/or to reduce the peak-to-peak value of the pitch link load time histories using harmonic IBC inputs. Closed-loop inputs of single and multiple frequencies were used to minimize various harmonic load

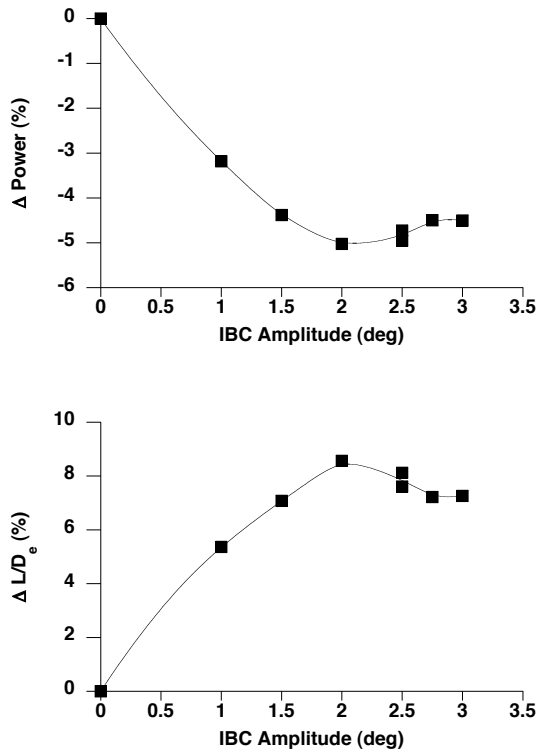


Figure 9. Power Reduction and L/D_e improvement for 2/rev manual IBC amplitude sweep (at 225° phase) with Trim Controller active, $C_L/\sigma=0.077$, $\mu=0.40$, $\alpha_S=-8.6^\circ$.

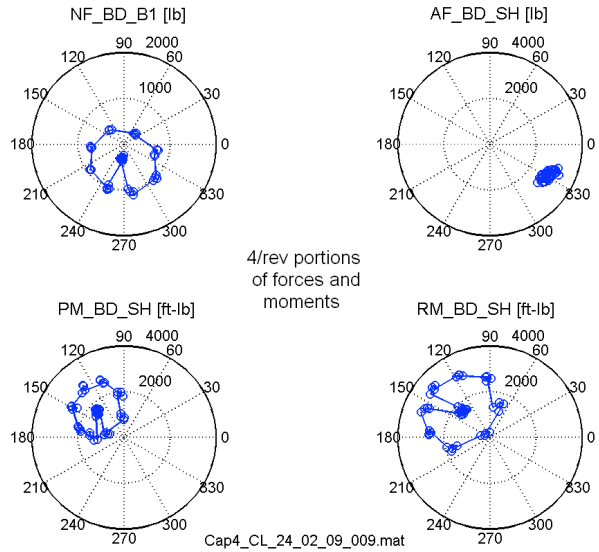


Figure 11. Impact of 4/rev IBC phase sweep (0.5° amplitude) on 4/rev hub loads (NF_BD_B1, AF_BD_SH, PM_BD_SH, RM_BD_SH), Lift=17,700 lb, $\mu=0.25$, $\alpha_S=-3.0^\circ$, Trim Controller active.

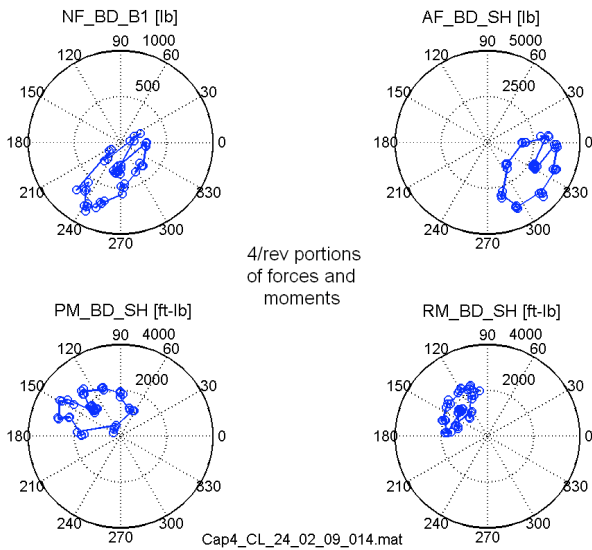


Figure 10. Impact of 3/rev IBC phase sweep (1° amplitude) on 4/rev hub loads (NF_BD_B1, AF_BD_SH, PM_BD_SH, RM_BD_SH), Lift=17,700 lb, $\mu=0.25$, $\alpha_S=-3.0^\circ$, Trim Controller active.

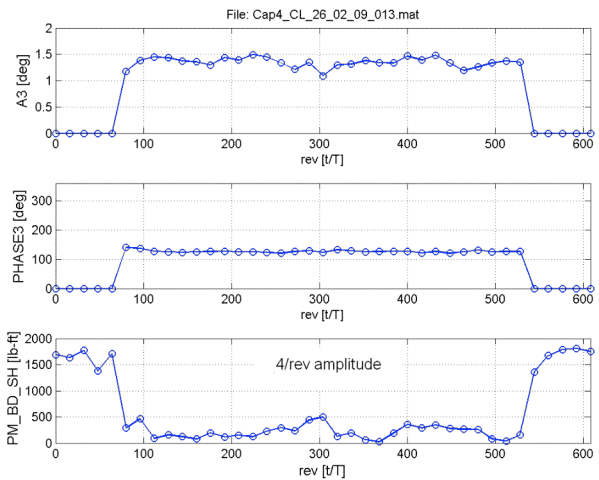


Figure 12. Closed-loop control performance for reduction of 4/rev hub pitching moment (PM_BD_SH) using 3/rev IBC, Lift=17,700 lb, $\mu=0.25$, $\alpha_S=-3.0^\circ$, Trim Controller active.

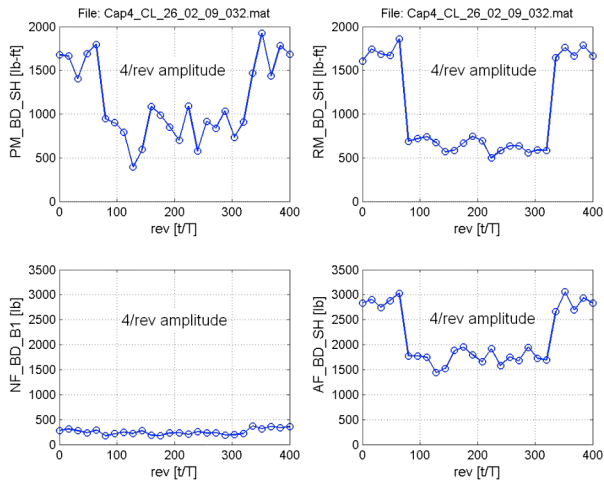


Figure 13. Closed-loop control performance for reduction of 4/rev portions of hub pitching and rolling moment (PM_BD_SH, RM_BD_SH), and normal force (NF_BD_B1) using 3+4/rev IBC. Uncontrolled hub axial force (AF_BD_SH) also shown, Lift=17,700 lb, $\mu=0.25$, $\alpha_S=-3.0^\circ$, Trim Controller active.

combinations. Testing was conducted at two different flight conditions including both high speed and high thrust conditions.

Figure 14 shows example open-loop results for one flight condition ($C_L/\sigma=0.077$, $\mu=0.35$, $\alpha_S=-7.4^\circ$). This figure plots the amplitude and phase values of the 2/rev and 4/rev pitch link loads of blade 1 for an IBC automatic phase sweep of 1° amplitude at a frequency of 2/rev. Similar data using 3/rev, 4/rev, and 5/rev inputs were acquired, from which a T-Matrix was identified recursively in real-time for subsequent closed-loop testing. Many closed-loop variations of input frequency and output harmonics were evaluated.

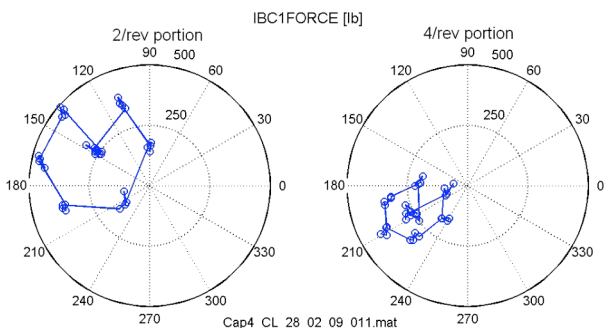


Figure 14. Impact of 2/rev IBC phase sweep (1.0° amplitude) on 2/rev and 4/rev portions of pitch link load (IBC1FORCE), $C_L/\sigma=0.077$, $\mu=0.35$, $\alpha_S=-7.4^\circ$, Trim Controller active.

Figure 15 shows the closed-loop results when minimizing 2, 3, and 4/rev harmonics of the pitch link load from one blade using 2, 3, and 4/rev IBC. The impact of IBC on two different pitch links are shown. In this case, the controlled harmonics are reduced significantly not only for the pitch link used to close the control loop (right side of Fig. 15), but also for the other pitch link which received the same (phase-shifted) commands (left side of Fig. 15). Nevertheless, the performance with respect to the controlled pitch link is slightly better. This indicates that it may be worthwhile to include the harmonics of more than one pitch link in the cost function of the controller.

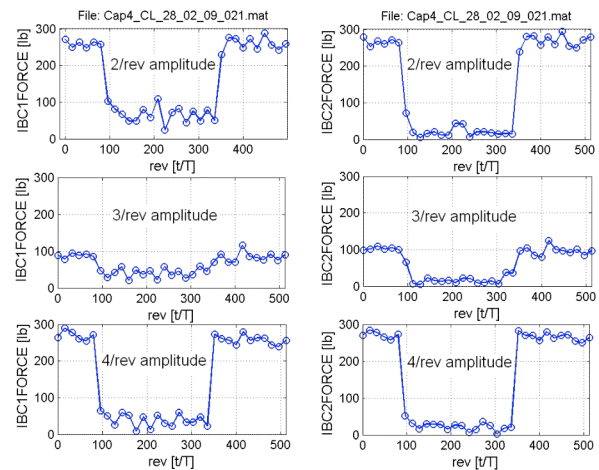


Figure 15. Closed-loop control performance for reduction of 2, 3, and 4/rev portions of pitch link loads (IBC1FORCE, IBC2FORCE) using 2+3+4/rev IBC, $C_L/\sigma=0.077$, $\mu=0.35$, $\alpha_S=-7.4^\circ$, Trim Controller active.

Figure 16 shows the pitch link load spectrum (up to 16/rev) with and without closed-loop IBC control. These data suggest that IBC is not decreasing specific harmonic components at the expense of increasing others. Only the 1/rev component is slightly increased over the non-IBC condition. The peak-to-peak values of the pitch link load time histories (not shown) were reduced approximately 20-30%.

In-plane Noise Reduction

The primary acoustic objective was to evaluate the ability of IBC to reduce rotor-generated in-plane noise. To accomplish this objective, open-loop single-frequency IBC phase sweeps from 2/rev-5/rev were conducted at three different flight conditions. Amplitude sweeps were then performed at those IBC phases showing the greatest acoustic benefit.

Figure 17 shows results from a limited 3/rev IBC phase sweep (1° amplitude) for one flight condition ($C_L/\sigma=0.077$, $\mu=0.35$, $\alpha_S=-7.4^\circ$). For this case, the negative acoustic peak

pressure that dominates low frequency harmonic content is shown to be reduced nearly 50% at an IBC phase of 230° for one of the in-plane microphones (Mic #9). Although additional data analysis is required at other microphones, flight conditions, and IBC frequencies, these results suggest that IBC can be beneficial for point reduction of in-plane noise.

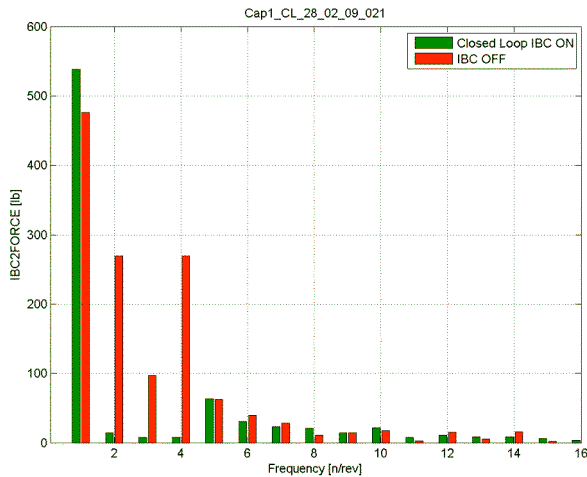


Figure 16. Spectrum of pitch link load (IBC2FORCE) with and without closed-loop IBC control, $C_L/\sigma=0.077$, $\mu=0.35$, $\alpha_s=-7.4^\circ$, Trim Controller active.

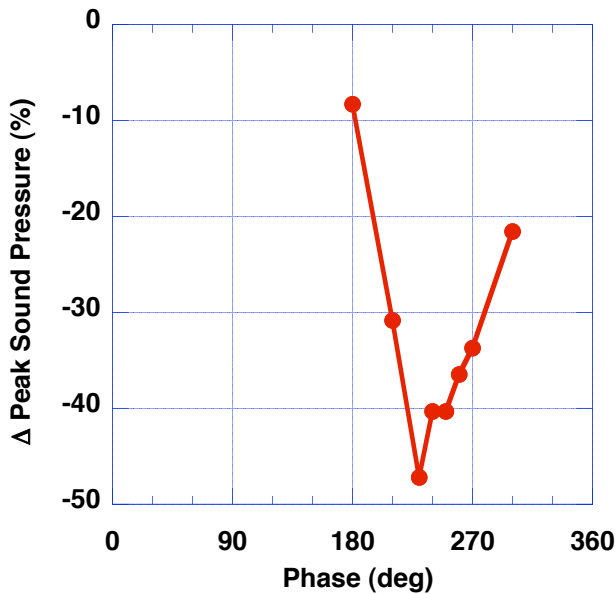


Figure 17. Reduction in peak sound pressure relative to baseline as a function of IBC phase (3/rev, 1° amplitude) for in-plane microphone (Mic #9), $C_L/\sigma=0.077$, $\mu=0.35$, $\alpha_s=-7.4^\circ$, Trim Controller active.

Flight Control Evaluation

The first of two flight control objectives was to evaluate and quantify the effect that IBC actuation for performance improvement and/or vibration/noise reduction has on the dynamic response of the UH-60A rotor system. To accomplish this objective, data were collected while dynamically exciting the rotor system through the swashplate at various test conditions with and without IBC actuation. Dynamic excitation was applied as frequency sweep commands individually to the swashplate collective, and longitudinal and lateral cyclic pitch inputs. Figure 18 shows an example of the control input and the rotor lift force and pitching moment responses for a baseline collective frequency sweep (no IBC). Two IBC actuation cases were considered in this experiment. One was representative of an open-loop IBC input that gives improvement in performance (2/rev IBC at a specific phase). The other was an open-loop IBC input that gives a reduction in vibration (3/rev IBC at a specific phase). Complete sets of frequency sweep records were collected at advance ratios of 0.25 (about 108 knots) and 0.35 (about 150 knots).

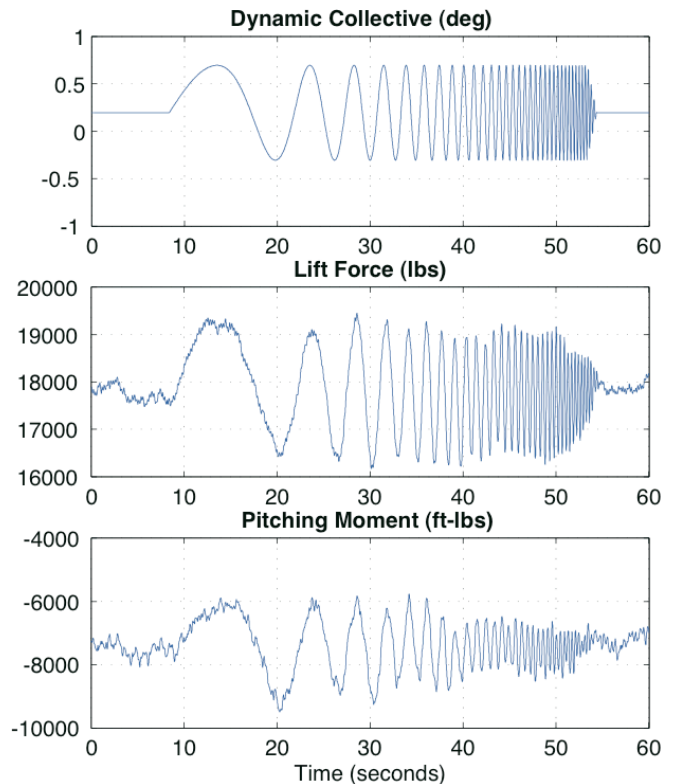


Figure 18. Sample control input and response for a collective frequency sweep.

Figure 19 shows the frequency responses of lift force due to swashplate collective with and without IBC actuation at an advance ratio of 0.25. The IBC actuation inputs were 1° , 2/rev actuation at a phase of 210° , and 0.5° , 3/rev IBC actuation at a phase of 0° . Comparisons of these and other frequency responses for cases with and without IBC actuation indicate how, and to what degree, rotor dynamics and rotor response are affected by IBC actuation. This single input/output pair comparison shows a slightly greater response magnitude near 0.7 rad/s for the IBC cases when compared to the baseline (no IBC) case. A more complete analysis is required to determine if this single result is representative of the effect of IBC on rotor dynamics. Future work is planned that involves identifying linear state-space dynamics models that include rotor and inflow dynamics for each test condition and for each IBC actuation input. The design and optimization of the primary flight control system would need to account for the effects of IBC if the inputs to the swashplate and IBC actuators produce a coupled response.

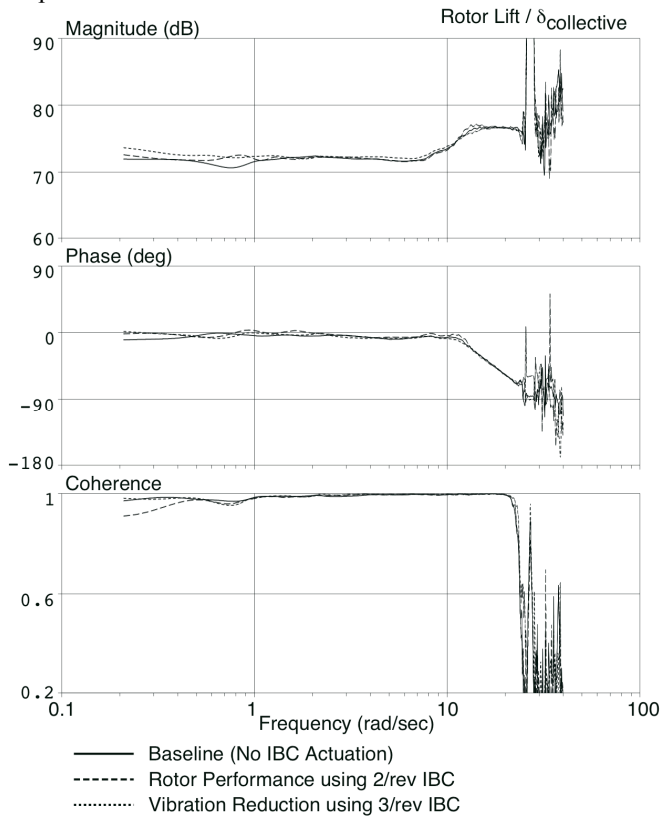


Figure 19. Sample frequency response of rotor lift due to swashplate collective with and without IBC input, $C_L/\sigma=0.077$, $\mu=0.25$, $\alpha_s=-3.0^\circ$.

The second flight control research objective was to determine if there are any adverse interactions or couplings between the closed-loop Trim Control System and the various closed-loop IBC configurations evaluated as part of

this wind tunnel test. This was accomplished by running the closed-loop IBC and Trim Control Systems concurrently at different operating conditions and with different closed-loop IBC configurations. This was important since if there were any interactions or couplings between the two control systems, then the individual systems would have had to be designed and optimized concurrently to minimize the impacts of one on the other. In all cases, there were no direct interactions observed between the two controllers that could be attributed to a coupling between the individual control responses. There was, however, some degradation in the performance of the trim controller over long time periods due to the fact that the trim control and IBC actuators shared the same hydraulic supply. This problem was simply fixed by terminating the trim controller, resetting the dynamic actuator control system and re-activating the trim controller.

Reconfiguration and In-flight Tuning

The Reconfiguration objective was to investigate the ability of IBC to counteract local (single blade) control system degradation. This degradation was simulated by using the IBC system to suppress the normal 1/rev motion of one blade. IBC was then used to apply counteracting (cyclic and/or collective) reconfiguration inputs individually at the remaining “unaffected” blades. Results from this effort are currently being analyzed.

The In-Flight Tuning objective was to demonstrate the ability of closed-loop IBC to reduce a 1/rev rotor imbalance in-flight using appropriate individual blade pitch offsets. Rotor imbalance conditions were simulated by application of two simulated blade defects/asymmetries. The simulated defects were 1) incorrect blade balance weight (removed weight from one blade), and 2) incorrect or modified blade trim tab setting (adjusted trim tab from nominal position). Testing was conducted at two different flight conditions for each simulated defect and two different tuning algorithms were evaluated at each flight condition. Before conducting the closed-loop tests, the IBC control system was configured to generate automatic open-loop blade pitch offset variations to identify the corresponding part of the T-Matrix model in real-time.

Figure 20 provides an example of closed-loop In-Flight Tuning results for the two tested flight conditions when an incorrect balance weight was simulated. The controller was configured to minimize the 1/rev harmonic of side force and pitching moment using blade pitch offsets of blade 1 and 2. The red horizontal lines represent the levels of reference vibrations without the deliberate imbalance condition (hence the balance condition for all other parts of the IBC test). It can be seen that the seeded failure or imbalance condition is of significant amount for both flight conditions. Moreover, it can be seen that the 1/rev vibration level at advance ratio $\mu=0.2$ can be reduced to the range of the reference level

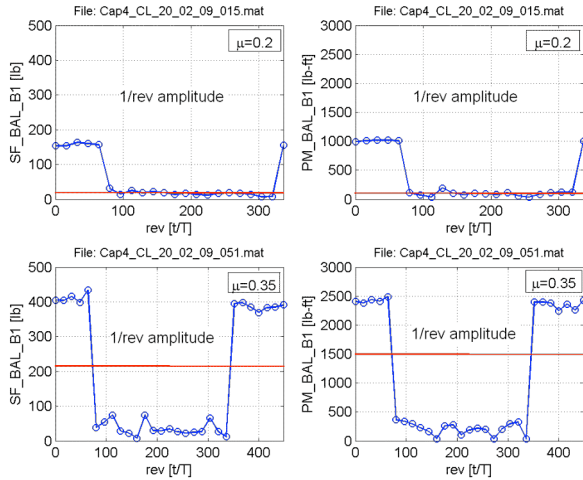


Figure 20. Closed-loop reduction of 1/rev portions of balance side force (SF_BAL_B1) and pitching moment (PM_BAL_B1) using blade pitch offsets on blade 1 and 2 at two different flight conditions, $C_l/\sigma=0.077$, $\alpha_s = -1.6^\circ$ or -7.4° (hub weight removed; red line is reference with no hub weight removed).

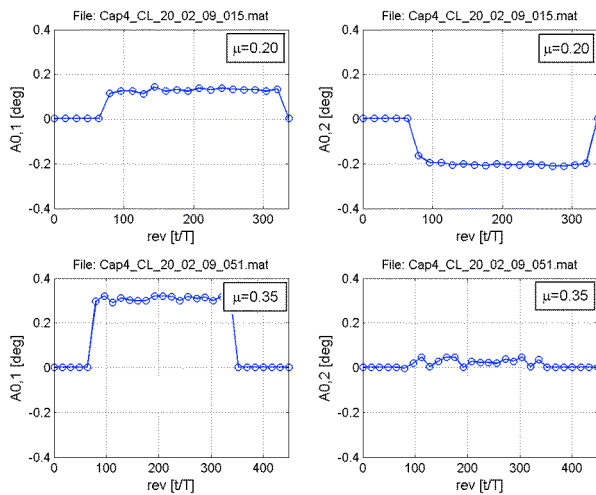


Figure 21. Commanded blade pitch offsets of blade 1 and 2 for closed-loop reduction of 1/rev portions of balance side force (SF_BAL_B1) and pitching moment (PM_BAL_B1) at two different flight conditions, $C_l/\sigma=0.077$, $\alpha_s = -1.6^\circ$ or -7.4° (hub weight removed).

(without simulated imbalance) during closed-loop operation. For the high-speed case, the closed-loop controller was able to reduce the 1/rev vibration level to near zero and hence to a level much smaller than the reference case. This is one indication of the benefit of an In-Flight Tuning capability, which ensures that for each flight condition an optimum 1/rev vibration condition can be achieved. Figure 21 shows that the required blade pitch offsets to achieve these results are different at the two flight conditions, once again

demonstrating the benefit of the In-Flight Tuning application. Similar results were found for other controller configurations and simulated blade defects (e.g. incorrect trim tab position).

CONCLUDING REMARKS

A full-scale wind tunnel test of a UH-60A rotor was recently completed in the NFAC 40- by 80-Foot Wind Tunnel to evaluate the potential of IBC to improve performance; to reduce vibration, loads, and noise; to affect flight control characteristics; and to perform reconfiguration and in-flight tuning tasks. This was the culmination of a collaborative wind tunnel test program between NASA, U.S. Army, Sikorsky Aircraft, and ZF Luftfahrttechnik GmbH (ZFL).

The initial test results included in this paper allow the following preliminary conclusions to be drawn:

- 1) Open-loop IBC inputs were shown to provide improved rotor performance. Power reductions up to 5% and L/D_e improvements up to 8.6% were found using 2/rev IBC inputs at high forward speed ($\mu=0.40$). The use of an automatic trim controller significantly improved the quality and efficiency of testing.
- 2) The IBC closed-loop controller was able to essentially eliminate single parameter, single frequency hub loads. When attempting to minimize multi-parameter, multi-frequency hub loads, however, a true closed-loop solution was not obtained due to load limitations on other parts of the model. Nonetheless, the results indicate that simultaneous reduction of multiple hub loads is possible with IBC.
- 3) The IBC closed-loop controller was able to simultaneously reduce multi-frequency pitch link loads with multi-frequency IBC inputs. These reductions were shown to have only a small effect on non-controlled pitch link harmonics.
- 4) Open-loop IBC inputs were shown to reduce the negative acoustic peak pressure that dominates low frequency harmonic content nearly 50% for one of the in-plane microphones. Although additional data analysis is required at other microphones, flight conditions, and IBC frequencies, these results suggest that IBC can be beneficial for point reduction of in-plane noise.
- 5) For one frequency sweep input/output pair (collective/lift), the presence of IBC actuation produced only a slightly modified response magnitude compared with the baseline (no IBC) case. A more complete analysis is required to determine if this single result is representative of the effect of IBC on rotor dynamics.

- 6) Closed-loop testing showed that a 1/rev rotor imbalance could be essentially eliminated using appropriate individual blade IBC offsets. The required blade pitch offsets to achieve these results were different at different flight conditions, thus demonstrating the benefit of the in-flight tuning capability.

APPENDIX

A more complete description of the Trim Control and IBC Control Systems is provided below.

Trim Control System

All of the functions of the Trim Control System, including the inner-loop trim control, mode switching and frequency sweep generator, were written in Matlab Simulink. The Simulink block diagram was compiled into an executable Dynamic Linked Library (DLL) using the Matlab Realtime Workshop toolbox. This executable library was then imported into National Instruments LabView and uploaded to the trim control hardware, which is a National Instruments PXI-1042Q real-time system with a PXI-8106 Embedded Controller. An operator interface to the trim controller ran on a separate desktop PC that was connected to the trim control hardware with an Ethernet cable. The trim control interface was developed in LabView and allowed the operator to control and monitor all aspects of the trim controller including the controller configuration, trim set point, controller operation and frequency sweep generator. The inputs to the Trim Control System were the rotor hub force and moment measurements from the DTC, available in near real-time. These rotor measurements were digitally low-pass filtered at 6Hz to remove the high-frequency rotor harmonic and vibration content before being used as feedback for the trim controller. The trim controller cycled at 100Hz, continually updating the swashplate position commands to achieve and maintain the desired trim condition. This hardware and software architecture allowed for rapid implementation of changes to trim control logic or the operator interface.

The control architecture for each of the trim control methods described earlier used PI (proportional and integral) control in each of the three swashplate control channels with the addition of a washout circuit in each channel to add damping and improve the overall performance of the controller. Cross-feeds were included between the swashplate collective pitch and longitudinal cyclic inputs to account for coupling between rotor lift and pitching moment in the first trim method, and rotor lift and propulsive force in the second trim method. An initial set of control law gains were calculated using the Control Designer's Unified Interface (CONDUIT) program (Ref. 17) based on a set of stability, performance

and disturbance rejection specifications. The rotor dynamic model used to calculate the control law gains was obtained using the FORECAST simulation code (Ref. 18). The control system gains were then tuned during initial wind tunnel testing to the final set of gains that were used during research data collection. Ultimately the desired controller performance at different wind tunnel and rotor loading conditions was obtained with a single set of gains for each of the control methods. This eliminated the need to schedule the control law gains with wind tunnel speed and rotor loading.

IBC Control System

Details on the hardware and software architecture of the IBC Control System as well as on the closed-loop algorithms are provided below.

IBC Control Architecture. Modifications necessary to incorporate the new IBC capabilities (IBC N/rev vibration control, individual blade 1/rev pitch commands, individual blade pitch offset commands) were accomplished with the development of a separate real-time control system, named Closed-Loop Hard & Software System (CLHSS). The resulting overall hardware control system architecture is depicted in Fig. 22. To link the new CLHSS to the existing IBC control system (middle part of Fig. 22), the latter has been expanded with a CL-CoLiFa System (Closed-Loop – Communication Limitation Fading System). Among other things this system provided an RS422-based serial communication interface to the CLHSS through which the CLHSS sent open- or closed-loop IBC command values to the IBC control system. To provide new IBC functionalities, like individual blade pitch offset commands, the underlying software of the IBC control system was modified.

The CLHSS was based upon a modular dSPACE hardware system and a corresponding Host-PC. The Host-PC was used for software development, software download and interaction with the real-time application. Based on the hardware control system architecture depicted in Fig. 22 the closed-loop control structure of Fig. 23 was implemented. The inner actuator position control loop (colored green in Fig. 22 and 23) was realized for each single IBC actuator by the corresponding actuator control boxes mounted in the rotating system. These control loops were built using analog techniques only. The actuator individual intermediate control loop of Fig. 23 was used to adjust the IBC command values (outputs of the outer control loop) in an adaptive manner to compensate for any remaining IBC amplitude and phase angle errors of the actuators. This loop was set up in the frequency domain and was based on fast/inverse fourier transforms (FFT/IFT). As indicated by the coloring in Fig. 22 and 23, this functionality was implemented within the IBC control system located in the non-rotating system (i.e. in the control room). These actuator individual intermediate control loops ensured that the offset, amplitude and phase

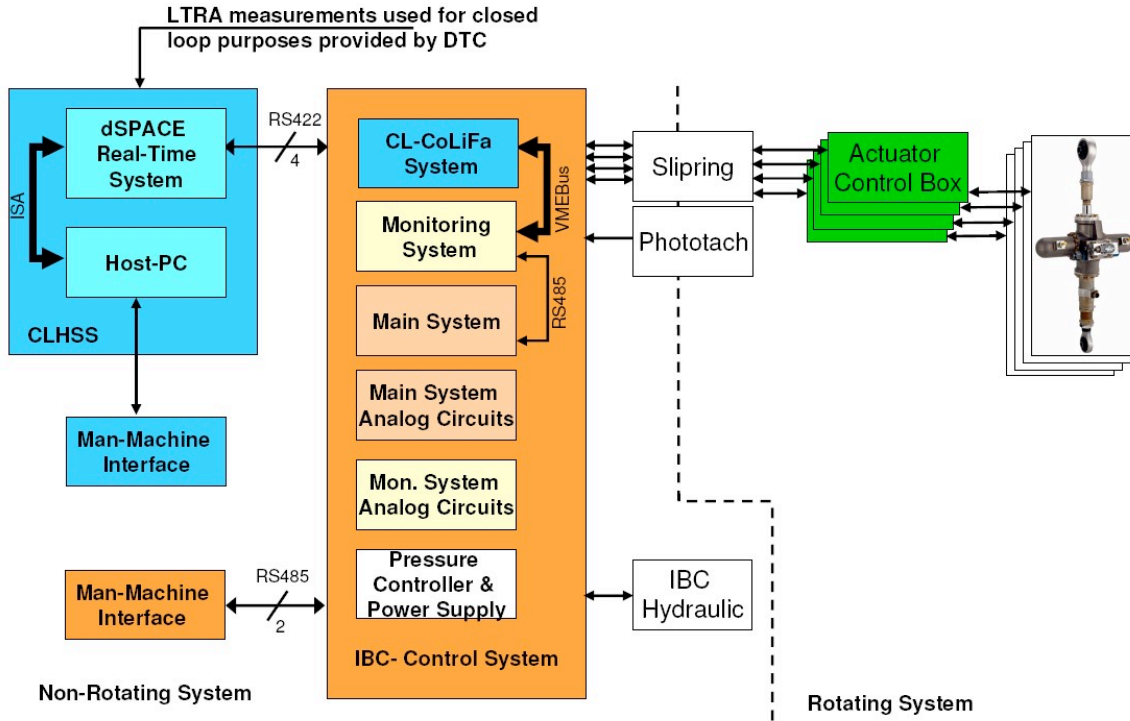


Figure 22. Hardware control system architecture of IBC System.

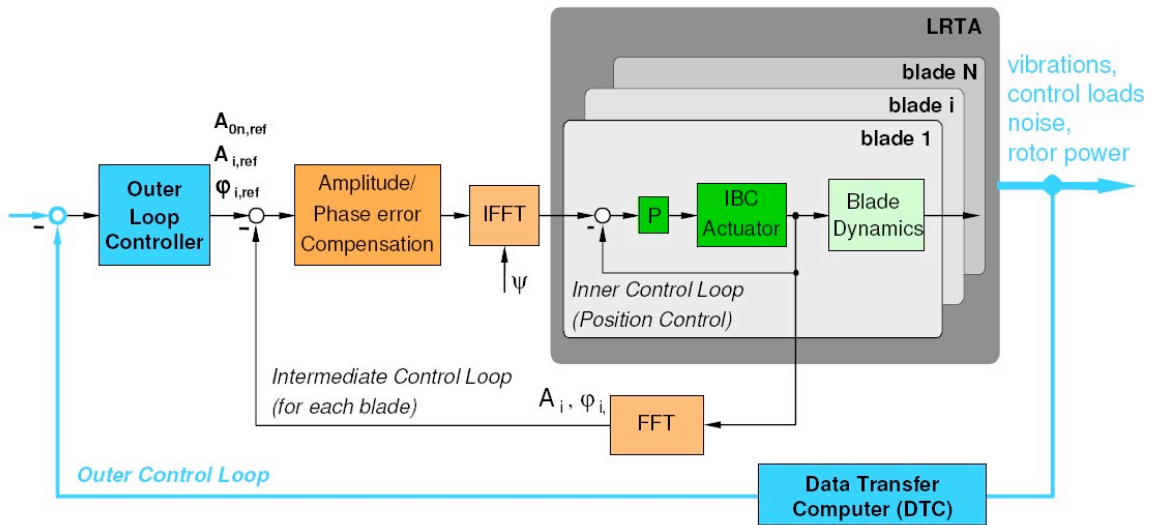


Figure 23. Block diagram of IBC closed-loop control structure.

control errors of each IBC actuator were very small and hence guaranteed that all actuators moved as commanded.

A third, outer control loop was added to this cascade architecture and thereby the IBC closed-loop control capability was realized. All outer control loop algorithms

were implemented on the CLHSS. To be able to close the outer control loop, the NASA DTC provided a subset of derived LRTA parameters in real-time as analog time histories to the CLHSS. The real-time software of the CLHSS provided the ability to generate open-loop as well as closed-loop IBC command values. These IBC command

values were transferred via the previously mentioned RS422-based serial communication interface to the IBC control system. The set of IBC command values was composed of individual blade pitch offsets, individual blade 1/rev amplitudes and phase, and 2/rev to 5/rev IBC amplitudes and phases.

Actuator travel versus command value was monitored by two completely independent systems (main and monitoring). As depicted in Fig. 22 the systems were functionally partitioned within the same physical package (a 19 in rack enclosure). The main system was designed to control the actuators by generating the command signals for the servo valves and performing the signal conditioning for 1 LVDT set (1 set corresponds to 4 LVDTs, 1 per actuator). The monitoring system was designed to perform monitoring duties and signal conditioning for the 2nd set of LVDTs. Failures could be detected by both systems with each having equal (highest) priority to trigger an emergency shutdown. Thus a redundant stroke monitoring was realized using 2 LVDT sensors for each actuator. When a certain actuator position control error was detected by at least one system or any other malfunction occurred, the hydraulic power was shut down. This immediately engaged the safety lock-out pistons and mechanically bolted the actuators in their zero positions. This feature made uncontrolled actuator travel nearly impossible. A shutdown signal was also generated when the measured axial load in any one of the actuators reached a preset threshold value.

The software of the outer control loop was developed using model-based design methods under Matlab Simulink. Based on the Simulink model the real-time code was automatically generated using Matlab Real-Time Workshop and the dSPACE Real-Time Interface (RTI). The closed-loop algorithms were partitioned into several tasks or subsystems that all together build up a Simulink Library. The overall controller model was realized without timer tasks. The fastest task (highest priority) was triggered by a hardware interrupt that was externally driven by the 128/rev signal. This hardware interrupt signal was generated within the IBC Open-loop System based on the phototach signal from the LRTA. Moreover, a 1/rev trigger signal was transmitted to the CLHSS for synchronization of all tasks with the tasks implemented on the IBC Open-loop hardware and with the rotor azimuth. All other interrupt driven tasks on the CLHSS were triggered by software interrupts. The sample times of the Controller and System Identification Tasks were easily modified by means of user-input parameters.

IBC Closed-Loop Control Algorithms. The closed-loop control algorithms used to form the outer control loop of Fig. 23 were based on the assumption that a quasi-static linear relationship between the outputs z (e.g. harmonic components of measured vibrations) and the corresponding set of IBC inputs ϑ described the plant behavior accurately

(linear T-matrix model, Ref. 12-16). The software within the CLHSS was setup for a T-matrix model

$$z_n = z_{n-1} + T_n (\vartheta_n - \vartheta_{n-1})$$

where

$$z \in \mathbb{R}^{69}, \vartheta \in \mathbb{R}^{24}, T \in \mathbb{R}^{69,24}$$

with

$$\vartheta = [\vartheta_{0,1}, \dots, \vartheta_{0,4}, \vartheta_{c1,1}, \vartheta_{s1,1}, \dots, \vartheta_{c1,4}, \vartheta_{s1,4}, \vartheta_{c2}, \vartheta_{s2}, \dots, \vartheta_{c5}, \vartheta_{s5}]^T$$

and

$$z = \begin{bmatrix} \cos 1_VIB1 \\ \sin 1_VIB1 \\ \vdots \\ \sin 5_VIB5 \\ \cos 2_PLL1 \\ \vdots \\ \sin 4_PLL2 \\ \text{mean_TORQ} \\ \text{mean_PWR} \\ \text{BVI_Signal} \\ \text{height_blade1} \\ \vdots \\ \text{height_blade4} \end{bmatrix}$$

The IBC input ϑ was composed of 1) the individual blade pitch offsets $\vartheta_{0,k}$ of blade $k=1$ through 4, 2) the individual blade 1/rev cosine and sine parts ($\vartheta_{c1,k}$ and $\vartheta_{s1,k}$) of blade $k=1$ through 4, and 3) the 2/rev – 5/rev components ϑ_{c2} thru ϑ_{s5} used for all blades. The output z was composed of 1) the 1/rev – 5/rev components of select rotor balance or hub loads, 2) the 2/rev – 4/rev (or 3/rev – 5/rev) components of loads from two pitch links, 3) the mean values of rotor torque and rotor power (averaged over a tunable number of rotor revolutions), 4) an acoustic signal and 5) the blade heights of all 4 blades. The blade heights were measured with a tracking camera that was installed permanently near the LRTA.

The overall outer control loop consisted of two main tasks: 1) a system identification task to estimate the linear T-matrix model recursively in real-time and 2) a controller task to calculate IBC inputs to accomplish the desired control task. The system identification task was performed using different Recursive Least Square (RLS) methods (standard RLS, RLS with forgetting factor, different stabilized RLS methods) or a Kalman filter-based implementation. Both local T-matrix

models and global T-matrix models were identified recursively within the implemented software.

With the controller task, two different controller methods were implemented. One closed-loop controller was realized by solving the following optimization problem (cf. also Ref. 19).

Minimize

$$J_{ctrl} = z_n^T W_z z_n + \vartheta_n^T W_\vartheta \vartheta_n + \Delta \vartheta_n^T W_{\Delta\vartheta} \Delta \vartheta_n$$

with respect to the identified T-matrix model

$$z_n = z_{n-1} + \hat{T}_n (\vartheta_n - \vartheta_{n-1})$$

where

$$W_z = \text{diag}(w_{z1}, \dots, w_{z36}) \in \mathbb{R}^{69,69},$$

$$W_\vartheta = \text{diag}(w_{\vartheta1}, \dots, w_{\vartheta12}) \in \mathbb{R}^{24,24},$$

$$W_{\Delta\vartheta} = \text{diag}(w_{\Delta\vartheta1}, \dots, w_{\Delta\vartheta12}) \in \mathbb{R}^{24,24},$$

$$\Delta \vartheta = \vartheta_n - \vartheta_{n-1}$$

and the subscript n denotes once more the current time step.

The solution of the above optimization problem was carried out only for a reduced set of system matrices and vectors to minimize the computational effort. The set of reduced matrices and vectors necessary to compute the optimum IBC inputs was chosen automatically according to the specification of the current control task (e.g. minimize or control 4/rev hub loads using a 3/rev IBC input). The way the software was implemented on the CLHSS allowed configuration of the closed-loop controller in an adaptive (i.e. with recursive system identification active during closed-loop control) or non-adaptive manner.

For the In-Flight Tuning application, a second closed-loop algorithm was implemented. This implementation was based on an optimization algorithm developed by the Rotor Track and Balance (RT&B) company, Helitune Ltd., and used within the German armed forces for the RT&B procedures of the CH-53G fleet. This algorithm was modified and tailored for the In-Flight Tuning application and integrated in the real-time code using the same model-based design techniques described earlier. Similar to the first control algorithm, this optimization algorithm made use of the same T-matrix model.

ACKNOWLEDGEMENTS

The authors gratefully acknowledge the significant efforts of the project partners (NASA, U.S. Army, ZFL, and Sikorsky) as well as the U.S. Air Force, in the planning, preparation, and execution of this current IBC test. Special

acknowledgement is made to Cahit Kitaplioglu, Alex Sheikman and Doug Lillie (NASA), Ben Sim (Army), Holger Witte and Karl-Heinz Bock (ZFL), and the entire Air Force/Jacobs Engineering test team, without whom this test would not have been successful. In addition, we wish to acknowledge the key people who kept this collaborative program alive over the years, including Steve Jacklin and William Warmbrodt (NASA), Andrew Kerr (U.S. Army), Axel Haber, Peter Richter, and Konrad Joecks (ZFL), and Gary de Simone (Sikorsky).

REFERENCES

1. Norman, T.R., Shinoda, P., Kitaplioglu, C., Jacklin, S.A., and Sheikman, A., "Low-Speed Wind Tunnel Investigation of a Full-Scale UH-60 Rotor System," American Helicopter Society 58th Annual Forum, Montreal, Canada, June 2002.
2. Jacklin, S.A., Haber, A., deSimone, G, Norman, T.R., Kitaplioglu, C., Shinoda, P., "Full-Scale Wind Tunnel Test of an Individual Blade Control System for a UH-60 Helicopter," American Helicopter Society 58th Annual Forum, Montreal, Canada, June 2002.
3. Jacklin, S. A., Blaas, A., Teves, D., and Kube, R., "Reduction of Helicopter BVI Noise, Vibration, and Power Consumption Through Individual Blade Control," American Helicopter Society 51st Annual Forum, Fort Worth, Texas, May 1995.
4. Lorber, P.F., Park, C., Polak, D., O'Neill, J., and Welsh, W., "Active Rotor Experiments at Mach Scale Using Root Pitch IBC," 57th Annual AHS Forum, Washington D.C., May 2001.
5. Arnold, U.T.P., "Recent IBC Flight Test Results from the CH-53G Helicopter," 29th European Rotorcraft Forum, Friedrichshafen, Germany, September 2003.
6. Cheng, R.P., and Celi, R., "Optimum Two-Per-Revolution Inputs for Improved Rotor Performance," *Journal of Aircraft*, Vol. 42, (6), November-December 2005, pp. 1409-1417.
7. Yeo, H., "Assessment of Active Controls for Rotor Performance Enhancement," *Journal of the American Helicopter Society*, Vol. 53 (2), April 2008, pp. 152-163.
8. Buckanin, R. M., Gould, W., Losier, P. W., Downey, D. A., Lockwood, R., Webre, J. L., Hagan, J. F., Cason, R. W., and Yourn, C. J., "Rotor Systems Evaluation, Phase I," AEFA Project No. 85-15, March 1988.

9. Kufeld, R.M., Balough, D.L., Cross, J.L., Stuebaker, K.F., Jennison, C.D., and Bousman, W.G., "Flight Testing of the UH-60A Airloads Aircraft," American Helicopter Society 50th Annual Forum, Washington D.C., May 1994.
10. Haber, A., Jacklin, S.A., and deSimone, G., "Development, Manufacturing, and Component Testing of an Individual Blade Control System for a UH-60 Helicopter Rotor," American Helicopter Society Aerodynamics, Acoustics, and Test and Evaluation Technical Specialists Meeting, San Francisco, CA, January 2002.
11. van Aken, J, Yang, L., "Development of a new State-of-the-Art Data Acquisition System for the National Full-Scale Aerodynamics Complex Wind Tunnel," 47th AIAA Aerospace Sciences Meeting, January 5-8, 2009, Orlando, FL.
12. Tischler, M.B., et al, "A Multidisciplinary Flight Control Development Environment and its Application to a Helicopter," IEEE Control System Magazine, Vol. 19, No 4, August 1999.
13. Kim, F.D., Celi, R., and Tischler, M.B., "High Order State Space Simulation Model of Helicopter Flight Mechanics," *Journal of the American Helicopter Society*, Vol. 38, No 2, October 1993.
14. Johnson, W., "Self-Tuning Regulators for Multicyclic Control of Helicopter Vibrations," NASA Technical Paper No. 1996, 1982.
15. Lehmann, G., Kube, R., "Automatic Vibration Reduction at a Four Bladed Hingeless Model Rotor – A Wind Tunnel Demonstration," *Vertica*, Vol. 14, No. 1, pp. 69-86, 1990.
16. Millot, T., Welsh, W., "Helicopter Active Noise and Vibration Reduction," 25th European Rotorcraft Forum, Rome, Italy 1999.
17. Fuerst, D., Auspitzer, T., Höfinger, M.T., van der Wall, B.G., "Numerical Investigation of Vibration Reduction Through IBC for a 20to Helicopter Rotor Model," 28th European Rotorcraft Forum, Bristol, England, 2002.
18. Fuerst, D. et al., "Closed Loop IBC-System and Flight Test Results on the CH-53 Helicopter," American Helicopter Society 60th Annual Forum, Baltimore, MD, 2004.
19. Arnold, U.T.P., Fuerst, D., "Closed loop IBC results from CH-53G flight tests," *Aerospace Sciences and Technology*, Vol. 9, pp. 421-435, 2005.